NASA/ TM-20250003078

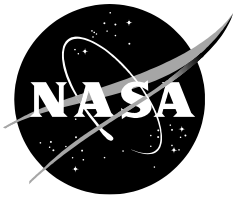

LISA-T part four: Low Earth Orbit Testing of Thin-Film Solar Array Materials

John A. Carr, Darren R. Boyd, and Miria M. Finckenor
Marshall Space Flight Center

March 2025

NASA STI Program Report Series

The NASA STI Program collects, organizes, provides for archiving, and disseminates NASA's STI. The NASA STI program provides access to the NTRS Registered and its public interface, the NASA Technical Reports Server, thus providing one of the largest collections of aeronautical and space science STI in the world. Results are published in both non-NASA channels and by NASA in the NASA STI Report Series, which includes the following report types:

- TECHNICAL PUBLICATION. Reports of completed research or a major significant phase of research that present the results of NASA Programs and include extensive data or theoretical analysis. Includes compilations of significant scientific and technical data and information deemed to be of continuing reference value. NASA counterpart of peer-reviewed formal professional papers but has less stringent limitations on manuscript length and extent of graphic presentations.

- TECHNICAL MEMORANDUM. Scientific and technical findings that are preliminary or of specialized interest, e.g., quick release reports, working papers, and bibliographies that contain minimal annotation. Does not contain extensive analysis.

- CONTRACTOR REPORT. Scientific and technical findings by NASA-sponsored contractors and grantees.

- CONFERENCE PUBLICATION. Collected papers from scientific and technical conferences, symposia, seminars, or other meetings sponsored or co-sponsored by NASA.

- SPECIAL PUBLICATION. Scientific, technical, or historical information from NASA programs, projects, and missions, often concerned with subjects having substantial public interest.

- TECHNICAL TRANSLATION. English-language translations of foreign scientific and technical material pertinent to NASA's mission.

Specialized services also include organizing and publishing research results, distributing specialized research announcements and feeds, providing information desk and personal search support, and enabling data exchange services.

For more information about the NASA STI program, see the following:

- Access the NASA STI program home page at http://www.sti.nasa.gov

- Help desk contact information:

https://www.sti.nasa.gov/sti-contact-form/ and select the "General" help request type.

NASA/ TM-20250003078

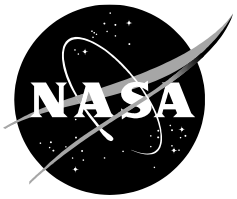

LISA-T part four: Low Earth Orbit Testing of Thin-Film Solar Array Materials

John A. Carr, Darren R. Boyd, and Miria M. Finckenor
Marshall Space Flight Center

National Aeronautics and
Space Administration

Marshall Space Flight Center
Huntsville, AL

March 2025

This report is available in electronic form at

https://ntrs.nasa.gov/

Corresponding Author:
Dr. John A. Carr
Deputy Center Chief Technologist, NASA MSFC Science and Technology
john.a.carr@nasa.gov | 256.763.2043 (m)

ABSTRACT

Satellite miniaturization continues to create lower cost, faster paced, and higher risk tolerant options for space missions. While very capable, the size of these small spacecraft has restricted both advanced missions as well as small spacecraft traveling deeper into space. To improve technical and distance capabilities, more work (i.e. sensing, processing, communication, power generation, etc.) must be done from less resources (i.e. mass, volume, surface area, etc.). This is a particularly difficult challenge for power generation. To achieve higher power generation without significantly affecting spacecraft size, mass, and volume, traditional solar array concepts are being adapted to fully thin-film assemblies. Many of the thin-film materials that are used in these assemblies have been tested to simulated space environments on the ground, but little data exist for on-orbit performance and survivability. Herein, results from an in-space materials exposure experiment are detailed. This mission was conducted on the 'Materials International Space Station Experiment Flight Facility' and included copper indium gallium (di)selenide solar cells, inverted metamorphic multijunction solar cells, as well as various coatings thereof. Current-Voltage data taken both before and after the mission exposure are presented and compared to ground test results to elucidate degradation mechanisms and recommend development needs to extend the lifetime of these thin-film photovoltaic assemblies.

KEYWORDS

LISA-T, MISSE-FF, MISSE-10, Solar, Thin-film, Photovoltaic, Cubesat, Small Spacecraft, Flexible, Space Environments Testing

1. INTRODUCTION

Satellite miniaturization continues to create lower cost, faster paced, and higher risk tolerant options for space missions [1-3]. Small spacecraft continue to grow in popularity and are of significant interest to government, scientific, exploratory, and commercial missions alike [4, 5]. NASA currently classifies small spacecraft or "SmallSat" to be spacecraft with a mass less than 180kg, which incorporates minisatellites, microsatellites, nanosatellites, picosatellites, and femtosatellites [1]. The large body of research and development within government, academia, and industry has greatly advanced small spacecraft technologies and, as a result, their mission capabilities [1-3]. However, the electrical power systems remain a bottleneck in small spacecraft bus design, mission capability, and operational distance from the sun. This drives the need for advanced power generation, storage, and distribution architectures.

To achieve higher power generation without significantly affecting the spacecraft resource allocation, traditional solar array materials and their supporting deployment mechanisms are being adapted to do more from less. One option to accomplish this is through the utilization of thin-film materials. The use of thin-film based solar arrays for spacecraft applications has long been recognized as an advantageous power generation option [6-11]. Thinner materials yield mass savings, equating to lighter launch loads and more payload allocation. Perhaps, more importantly for small spacecraft, their mechanical flexibility lends itself well to advantageous stowage and deployment designs. These benefits make thin-film arrays an exciting prospect to solve the inherent small spacecraft challenges discussed above. Though several larger scale thin-film or partial thin-film arrays are in development [12], sub-kilowatt thin-film arrays – optimized for small spacecraft – remain in need. The Lightweight Integrated Solar Array and anTenna (LISA-T) (**Figure 1**), being developed at NASA's George C. Marshall Space Flight Center [13-15], seeks to fill this technology gap.

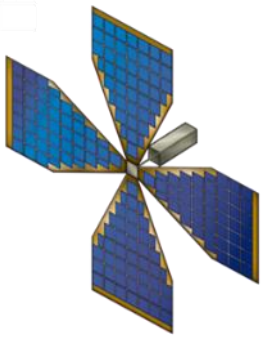

Figure 1: Depiction of LISA-T planar array configuration.

The LISA-T array has been ground tested to 'Technology Readiness Level 6', meaning subsystem prototypes have been tested in relevant, simulated space environments such as particulate radiation, thermal cycling, atomic oxygen, and the like [15]. To better understand these results as well as to further build an operational performance and survivability model, a Low Earth Orbit (LEO) exposure test was conducted. The Materials International Space Station Experiment Flight Facility (MISSE-FF) was utilized for this experiment. The MISSE-FF is a modular and robotically serviceable external facility that is located on the International Space Station (ISS) Express Logistics Carrier-2 Site 3 (ELC-2 Site 3) [16]. It provides ram, wake, zenith, and nadir exposures in the LEO environment at the ISS altitude [16]. Samples are sent and installed in the flight facility and are later retrieved and returned to Earth for further study. Of significant advantage to MISSE-FF is that samples are exposed to the true, *combined* environments of space – i.e. particulate radiation simultaneously *with* thermal cycling, atomic oxygen, ultraviolet radiation, and the like. This contrasts to the typical single, *sequential* exposure of ground testing – i.e. particulate radiation *then* thermal cycling, atomic oxygen, ultraviolet radiation, and the like. Herein results from the MISSE-FF mission comprising LISA-T core materials, solar cells, and stack-ups thereof are detailed.

2. EXPERIMENTAL SETUP

Figure 2 depicts the LISA-T MISSE-FF mission plate. In total, 25 samples were tested. Group (a) are bare and witness materials including CORIN XLS with a glass additive, Novaclear with a polyhedral oligomeric silsesquioxanes (POSS) additive, Optinox SR with POSS additive, and a Kapton covered radiation dosimeter. Group (b) are copper

indium gallium (di)selenide photovoltaic devices (supplied by Ascent Solar) [17]; bare cells as well as cells coated with CORIN XLS, CORIN XLS with ceria additives, and CORIN XLS with glass additives were included. Lastly, group (c) are inverted metamorphic multijunction (IMM) photovoltaic devices (supplied by Microlink Devices) [18]; bare cells as well as cells coated with Optinox SR and Optinox SR with a POSS additive were included.

Figure 2: LISA-T MISSE-FF mission plate (a) bare materials and witness samples, (b) copper indium gallium (di)selenide solar cells, (c) inverted metamorphic multijunction solar cells.

The LISA-T MISSE-FF plate flew for 1-year on the Zenith facing side of the carrier during the MISSE-10 mission. The experiment was completely passive, meaning performance and other key measurements were made in the lab both pre and post Zenith exposure; no active measurements were made on-orbit. The mission plate spent a total of 6,000.9 hours opened and exposed, with some of that time in sun, some in eclipse, and some in a solar shadow caused by the flight facility orientation. The MISSE sample carriers were closed during visiting vehicle operations, to minimize contamination; however, the LISA-T samples remained under the vacuum of space and experienced some thermal cycling and particulate radiation exposure, but no Ultraviolet (UV) or Atomic Oxygen (AO) exposure, during these times. **Table 1** summarizes the estimated material exposures per relevant environment.

Table 1: MISSE-10 LISA-T Mission Plate Environmental Exposure Summary

Environment	Estimated Exposure	Source
Ground Exposures		
Bake Out	60°C for 24hrs at 10^{-6} Torr	Lab, as measured in chamber
Humidity	<50% Relative, <24 hours exposure	Lab, tracked by humidity sensors
On orbit Exposures		
1MeV-eq Electron Radiation	~4.40×10^{12} e-/cm^2 1MeV equivalent	LEO, as estimated by SPENVIS, includes electrons, trapped proton, and solar proton components
100keV Proton Radiation	~ 6.40×10^{10} p+/cm^2	LEO, as estimated by SPENVIS, single low energy breakout given for reference
Ultraviolet Radiation	~3,000 ESH	LEO, as estimated by solar exposure measurement and shadow modeling
Atomic Oxygen	1.66×10^{20} atoms/cm^2	LEO, as measured by Kapton Witness
Thermal Cycling	~5,840 cycles -40 to +40°C	LEO, as measured on mission plate

Environments were either directly measured or estimated based on modeling data. The bake out environment was directly measured as run in the ground chamber. Relative Humidity (RH) exposure was minimized, but not eliminated. The approximate exposure was estimated by using RH sensors as samples were open in the laboratory environment. Note, once integrated to the mission plate, the assembly was stored in a nitrogen purge bag. It remained in this bag through spacecraft integration, launch, and delivery to the ISS. Total radiation dose was measured on orbit via a dosimeter which was included on the LISA-T plate (**Figure 3**) and was further broken out into estimated electron and proton components via the SPENVIS [19] modeling suite. The 1MeV equivalent electron fluence is used for analysis herein and includes the total electron contribution, the total trapped proton contribution, as well as the solar proton contribution as defined by SPENVIS. Ultraviolet radiation has components of both measurement and estimation. The plate's solar exposure was tracked and measured on orbit, however, shadowing from ISS components and the MISSE-FF also occurred and was accounted for via modeling. Atomic oxygen was measured directly by utilizing a Kapton witness (**Figure 3**). The atomic oxygen erosion of Kapton is well known [20, 21] and pre/post measurements of the witness sample enabled determination of the mission exposure. Lastly, thermal cycles were measured on orbit directly on the mission plate via thermocouple devices.

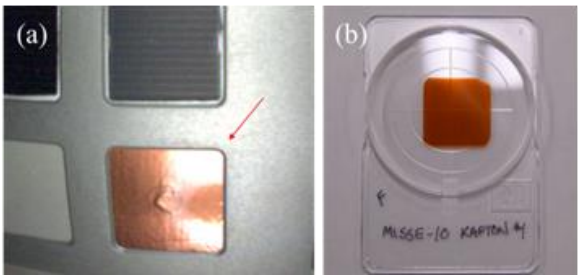

Figure 3: Images of dosimeter + Kapton witness setup (a) on orbit via the flight facility camera and (b) post flight laboratory image.

3. MEASURED RESULTS

Figure 4 shows the pre and post images of the LISA-T MISSE mission plate. Many coloring differences can be observed in the material groups as well as the metal plate itself.

Figure 4: Pre-flight (a) and post-flight (b) images of the LISA-T flight plate.

CIGS Solar Cells

Figure 5 shows sample pre- (a) and post- (b) images of the CIGS assemblies: (i) bare CIGS, (ii) CIGS with CORIN XLS, (iii) CIGS with CORIN XLS and glass nanoparticle additives, and (iv) CIGS with CORIN XLS and ceria additives.

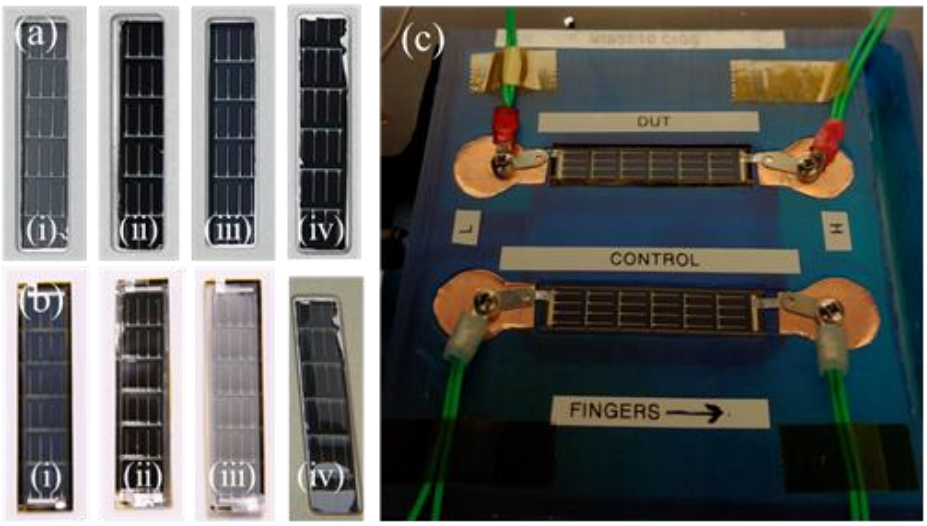

Figure 5: Pre- (a), post- (b) flight, and device under test (c) of the CIGS MISSE samples. (i) is a bare CIGS cell, (ii) CIGS with CORIN XLS, (iii) CIGS with CORIN XLS and glass nanoparticles, and (iv) CIGS with CORIN and Ceria additives.

Figure 6 shows pre- and post-IV curves for each of the CIGS assemblies. Measurements were taken on 4-wire Air Mass-0 setup (**Figure 5**c) which was carefully controlled via three mechanisms. First, the spectral components and integrated intensity of the light source were controlled via measurement from a spectroradiometer. Second, each individual measurement was controlled with a simultaneous, real-time measurement of a 'control' solar cell to monitor test-by-test fluctuations. Finally, witness samples were maintained for each flight solar cell and were also measured as Devices Under Test (DUTs). These witness samples saw all the same ground environments as well as the same handling as the flight samples – the key difference being that they were stored under nitrogen while the flight samples were exposed in space. This allowed pre- and post-IV differences to be isolated to the space environments and gave further control on the I-V measurements. **Table 2** summarizes the primary results of these measurements.

Table 2: Degradation data for LISA-T MISSE flight assemblies. The percentages represent post divided by pre. 3x samples measured for each.

	P_{max}	I_{sc}	V_{oc}	FF	Coating Thickness
CIGS Bare	77.5%	96.0%	96.3%	83.8%	0μm
CIGS CORIN XLS	92.2%	98.6%	98.3%	95.1%	12.3μm
CIGS CORIN XLS w/ Glass additive	92.1%	90.4%	101%	100%	24.9μm
CIGS CORIN XLS w/ Ceria additive	86.6%	92.3%	96.7%	97.1%	11.0μm
IMM Bare	78.3%	94.5%	90.6%	91.3%	0μm
IMM Optinox SR	79.0%	80.1%	98.2%	100.4%	20.4μm
IMM Optinox SR w/ POSS additive	77.0%	75.1%	96.8%	105.9%	27.5μm

In **Figure 6a** a large degradation of the bare CIGS device can be observed. Degradation in short circuit current (I_{sc}), open circuit voltage (V_{oc}), fill factor (FF), and, thereby, max power (P_{max}) is noted (**Table 2**), with ~77.5% output power reaming after the LEO flight. The addition of both CORIN XLS as well as CORIN XLS with glass to the modules significantly increased the power remaining to ~92% (**Figure 6b, c)**. Unexpectedly in comparison, the addition of CORIN XLS with ceria showed a more modest improvement to 86.6% (**Figure 6d)**.

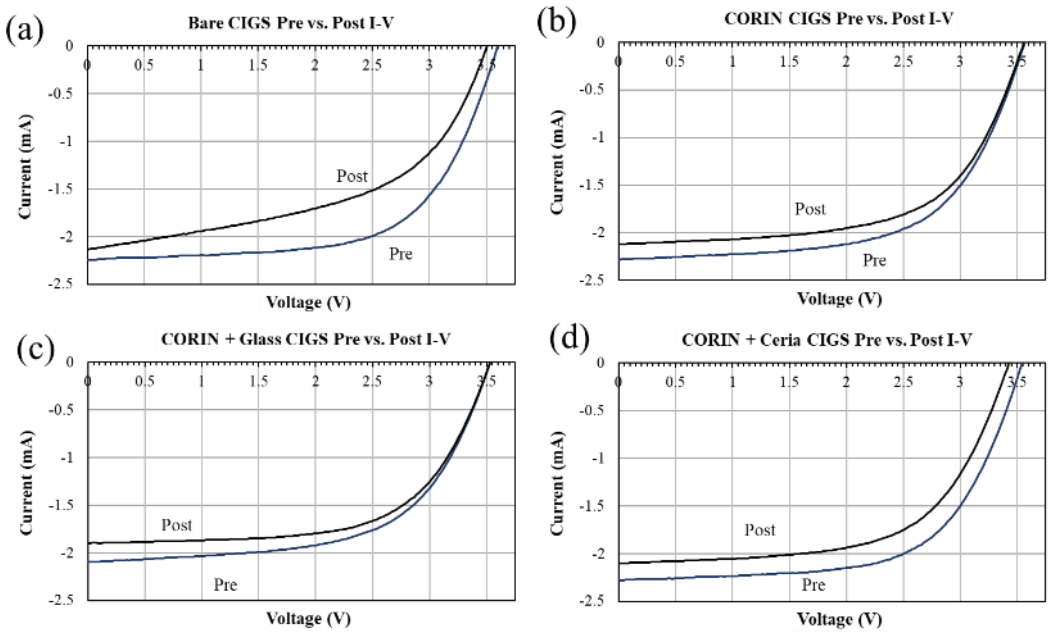

Figure 6: Pre- and Post-flight I-V data for (a) bare, (b) straight CORIN, (c) CORIN with glass additives, and (d) CORIN with ceria additives.

Utilizing the environments defined in **Table 1** as well as the ground testing results in ref [15] the primary causes of the on-orbit degradation profile can be understood. The humidity exposure was proven to be of little consequence through the witness samples, which saw the same humidity environments but displayed no degradation. It is worth noting though, that longer exposures to higher humidity levels can indeed degrade CIGS modules [15]. Similarly, it is expected that the thermal ranges seen during the ground bakeout as well as those through on orbit cycling were also benign to the CIGS assemblies. While the exact, lowest *beneficial* thermal treatment temperature is currently not known, it is known that post manufacturing treatment as well as post radiation thermal exposure at temperatures as low as 100°C actually *improve* performance and, more importantly here, it is not until much higher temperatures that performance is degraded [15]. It is unclear if the 40-60°C temperature exposure benefitted the assemblies but is not expected to have contributed to any degradation. The modest electron radiation levels seen during the MISSE exposure (~4.40×10^{12} e-/cm^2 1MeV equivalent) were also not expected to have significantly affected the CIGS modules, as can be seen in figure 15 of ref [15]. In fact, it is not until fairly high fluences, >5×10^{14} e-/cm^2 1MeV equivalent dose, that degradation is noted [15]. This radiation robustness of CIGS has also been reported elsewhere [22, 23]. The same is expected for proton radiation. While the current model of trapped protons does not include highly damaging energies below 100keV, it is expected that the total fluence at these low energies is well below the 1×10^{12} p+/cm^2 where bare CIGS modules begin to degrade. Further, ref [15] shows that the thin-film coatings used herein are robust enough to block proton energies <~800keV and protect cells through reasonably high fluences. UV, however, has a significant effect on CIGS modules, as seen in ground testing (figure 23 of ref [15]). And, as will be shown below, AO exposure is also thought to have significantly contributed to the degradation on the bare modules.

Bare CIGS Modules: **Figure 7** shows the I-V of a representative bare CIGS module through accelerated ground testing of UV exposure (230 to 400 nm at ~1 to 1.6x equivalent suns). Notably, the degradation of the short circuit in the ground tested base CIGS cells was ~3-4% after nearly 3,000 equivalent sun hours (ESH) UV exposure, closely matching that of the I_{sc} degradation of the flight samples. This likely accounts for the current loss seen on the MISSE flown samples.

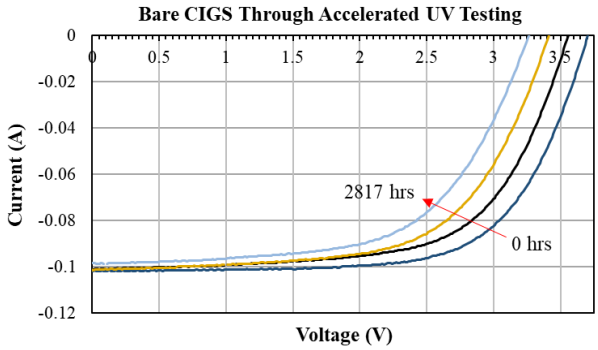

Figure 7: I-V data of a bare CIGS solar cell through accelerated ground testing of UV exposure.

Conversely, the open circuit voltage of the MISSE flown bare CIGS module was significantly *less* degraded with the fill factor significantly *more* degraded than is explained by UV exposure alone, indicating additional, concurrent effects (**Figure 6a** compared to **Figure 7**). The FF is likely a result of AO exposure and resulting erosion and/or oxidation of the top layers including electrode fingers. AO has not been directly tested on bare CIGS modules, however, visual erosion and evidence of oxidation on the flight samples is consistent with that of samples left open for extended exposure in the laboratory as well as samples put through an intentional, high relative humidity exposure ground test. **Figure 8a** shows an enlarged view of a MISSE flown bare CIGS sample, with the red arrow highlighting a particularly noticeable area of erosion and oxidation. **Figure 8b** shows I-V data for ground tested bare CIGS cells held through 80% relative humidity (RH) and 27°C for a 10-day exposure. Coloring change and oxidation evidence similar to **Figure 8a(i-ii)** was noted in this ground test. **Figure 8b** shows degradation only in the FF, consistent with increased solar cell resistances and gives supporting evidence explaining the additional FF decrease of the flight samples.

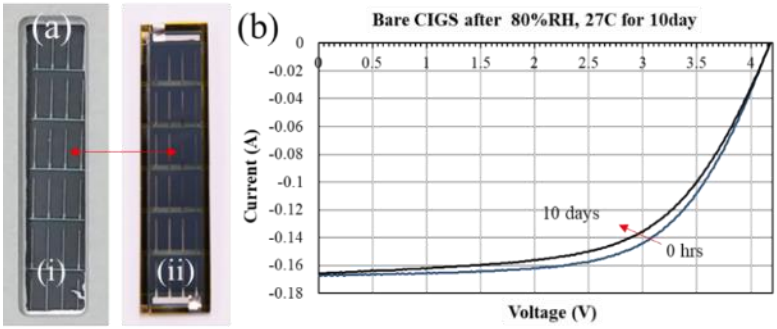

Figure 8: (a) MISSE bare CIGS sample (enlarged) pre- (i) and post-flight (ii). (b) Representative I-V response of bare CIGS grounded tested in 80% RH, 27°C for 10 days.

The reasoning behind the unexpectedly lower degradation of the flight sample V_{oc} is unknown. It is speculated that the 60°C upper temperatures seen are orbit are enough to anneal benefit the V_{oc}, however, this has not yet been attempted in a laboratory test.

Coating the bare CIGS assembly with both CORIN XLS as well as CORIN XLS with glass additives significantly improved the LEO environmental stability of the CIGS module. Both coatings showed ~92% power reaming after flight, however, the different coatings showed different degradation profiles. As seen in **Table 2**, CORIN XLS showed modest degradation across all three I-V components while CORIN XLS with glass showed degradation only in I_{sc} with a slight increase in V_{oc}.

CORIN XLS CIGS Modules: **Figure 9** shows I-V data for a representative CORIN XLS coated CIGS assembly though accelerated ground testing of UV. When compared to bare modules in **Figure 7,** V_{oc} and FF degrade significantly less during the same period. This is due to the protection given by the coating, which absorbs a significant portion of the

CIGS damaging UV. However, because of this UV absorption, a yellowing of the CORIN polyimide occurs, decreasing transmission and the I_{sc} of the module. Advantageously, The I_{sc} on coated assemblies degrades much more slowly than the V_{oc} and FF on uncoated cells, yielding a net benefit through the coating. It is expected that some components of the UV band still reached the MISSE flight CORIN XLS modules given the relatively thin coating (~12.3µm), contributing to the V_{oc} and FF losses observed. CORIN XLS also gives excellent protection against Atomic Oxygen [24], negating the erosion and oxidation effects seen on the FF of bare modules. As observed in **Figure 5-ii** no significant visual difference was seen pre- versus post-flight, in stark contrast to the bare modules.

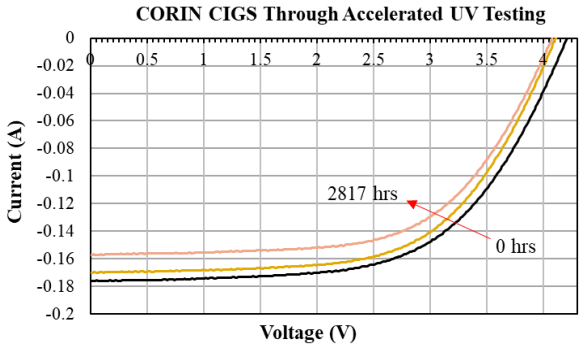

Figure 9: I-V data of a CORIN XLS coated CIGS module through accelerated ground testing of UV exposure.

The FF degradation of the CORIN XLS CIGS modules can be explained entirely by UV exposure, however, both the I_{sc} and V_{oc} cannot. The I_{sc} of the flight CORIN XLS CIGS samples degraded significantly less than expected based on ground testing in solely UV exposure – ~90.1% I_{sc} remained after ground testing while ~98.6% remained on orbit. This difference is attribute to net positive, synergistic effects of AO erosion. While CORIN does not erode rapidly, it erodes nonetheless and it is believed that as the UV yellows the top layers of the CORIN film, the AO subsequently erodes some of this damage away, causing the degradation on orbit to significantly lag that of UV-only testing on the ground. The V_{oc} on orbit also degraded modestly *less* than UV-only ground test samples – ~96.4% remained after UV ground testing while 98.3% remained on orbit. This is consistent with the lower overall V_{oc} degradation observed from the bare CIGS modules and requires further investigation.

CORIN XLS w/ glass CIGS Modules: While CORIN XLS with glass additive coated CIGS modules showed a similar end P_{max} to that of straight CORIN XLS (**Table 2**), the I-V performance details differed. The FF of the CORIN XLS with glass showed no change and V_{oc} the showed modest improvement. This variance is believed to stem from the unintentional thickness difference of the coatings. It is likely that the additional thickness of the glass doped CORIN XLS (24.9µm) blocked more UV and, thereby, further protected the FF and V_{oc}. It is theorized then that thicker coatings of straight CORIN XLS would achieve similar results. The improved V_{oc} is again observed consistent with bare and straight CORIN modules, with this assembly reaching 101% on the post measurement.

The I_{sc} of the glass doped CORIN XLS, however, significantly lagged that of straight CORIN XLS. Two mechanisms are suspected. First, the thicker coating absorbs more UV and yellowed more significantly, decreasing transmission and, thereby, $I_{sc.}$ Secondly, and more importantly, a clear visual difference can be seen in the pre- and post-flight module images (**Figure 10**). A hazing is observed and attributed to an interaction between the glass nanoparticles and AO. This hazing is reducing light transmission and, thereby, I_{sc}.

Figure 10: Enlarged view of Pre- (a) and Post-flight (b) images of CORIN XLS with glass additive coated CIGS modules.

CORIN XLS w/ ceria CIGS Modules: The CORIN XLS with ceria additive coated CIGS modules showed anomalous behavior when compared to straight CORIN XLS as well as CORIN XLS with glass; however, more closely matched ground tested modules. **Figure 11** shows accelerated ground testing of CORIN XLS with ceria coats modules through UV. The degradation profile is consistent to that of the MISSE flight assemblies with the same coating. When compared to both straight CORIN XLS as well as CORIN XLS with glass flight samples, however, the CORIN with ceria modules did not show the improved V_{oc} when compared to their ground tested counter parts.

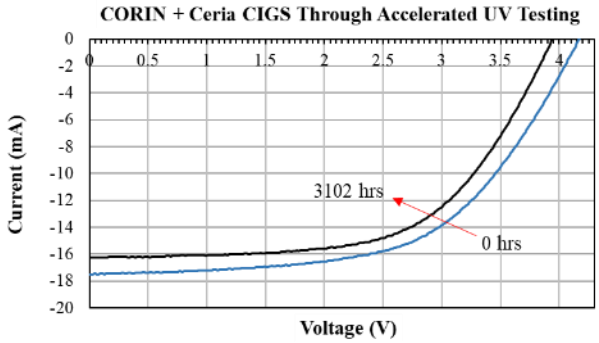

Figure 11: I-V data of a CORIN XLS with ceria additives coated CIGS module through accelerated ground testing of UV exposure.

IMM Solar Cells

Figure 12 shows sample pre- (a) and post- (b) images of IMM solar cell assemblies: (i) bare IMM, (ii) IMM with Optinox SR, and (iii) IMM with Optinox SR and POSS additives. IMM samples were measured and controlled (**Figure 12c**) in the same manner as the CIGS modules.

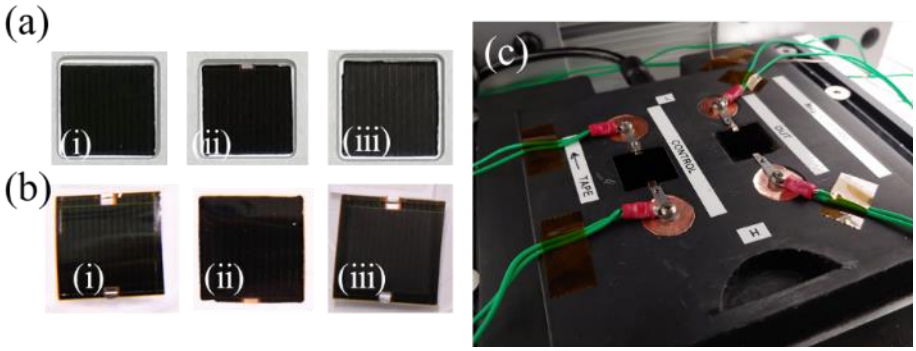

Figure 12: Pre- (a), post- (b) flight, and device under test (c) of the IMM MISSE samples. (i) is a bare IMM cell, (ii) IMM with Optinox SR, and (iii) IMM with Optinox SR with a polyhedral oligomeric silsesquioxanes additive.

Figure 13 shows pre- and post-flight 4-wire IV curves for each of the IMM assemblies. Clear degradation in all three assemblies is observed. Per **Table 2**, all three assemblies degraded to a very similar end state through the flight experiment – ~77% to 79% P_{max} remaining. However, the degradation profile of both the Optinox SR as well as the Optinox SR with POSS assemblies differed significantly from that of the bare IMM. Revisiting the environments defined in **Table 1** as well as the ground testing results in ref [15] the primary causes of on-orbit degradation can be understood.

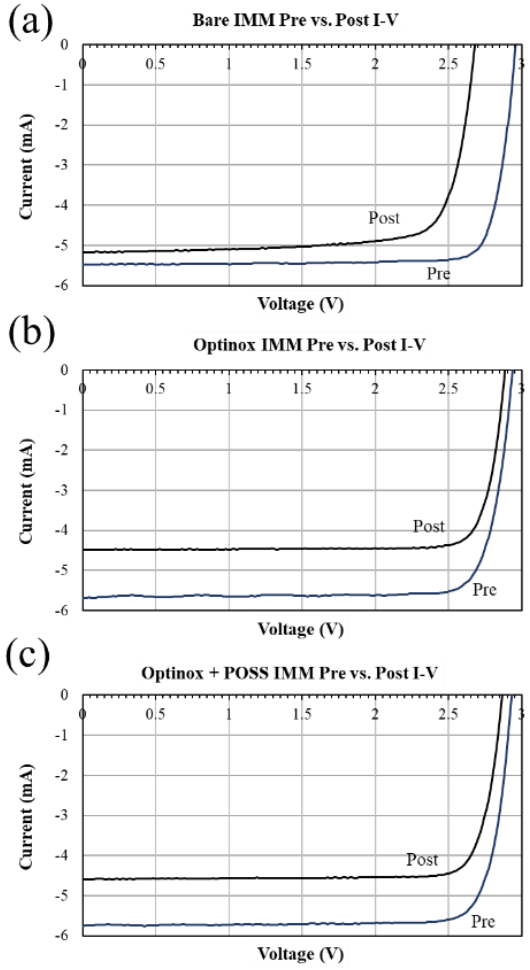

Figure 13: Pre- and Post-Flight I-V data for (a) bare, (b) straight Optinox, and (c) Optinox with POSS.

Consistent with the CIGS assemblies, the humidity exposure was proven to be of little consequence through the witness sample measurements, which saw the same humidity environments but displayed no degradation. It is also expected that the thermal ranges seen during bakeout as well as on orbit were also benign to the IMM cells. As can be seen in figures 17 and 19 of ref [15], the IMM cells can survive temperatures as high as 170°C without degradation and, much like the CIGS modules, even exhibit performance *improvement* with post radiation annealing at least as low as 100°C. It is again unclear if the 40-60°C temperature exposure benefitted the assemblies but is concluded the thermal exposure did not significantly contribute to any degradation. Also similar to the CIGS modules, the modest electron radiation levels seen during the MISSE exposure (~4.40×10^{12} cm^{-2} 1MeV equivalent) is not expected to have significantly affected the IMM assemblies, as can be seen from the ground testing in figure 15 of ref [15]. However, in contrast to CIGS modules, the bare IMM cells are significantly more susceptible to low energy proton damage, at least at fluences of ~7×10^{10} cm^{-2} and likely lower depending on energies [15]. Also in contrast to CIGS modules, the bare IMM is not influenced by UV, however, the Optinox SR coating is expected to yellow under exposure, as seen in figure 23 of ref [15]. Lastly, AO is known to affect the bare IMM as observed in figure 14 of ref [15], but, again, the coatings are expected to provide sufficient protection and even showed some improvement after more significant AO exposure (>1.4×10^{21} cm^{-2}) [15].

Bare IMM: The bare flight cells showed a significant drop in both V_{oc} and FF after the LEO exposure, while the I_{sc} showed a somewhat more modest degradation (**Table 2**). Low-energy, trapped proton radiation is expected to primarily constitute this degradation with a small contribution from neutral AO. **Figure 14** shows I-V curves for

ground tested bare IMM through two fluences of 50keV protons. Note, this is only a single energy test whereas on orbit *multiple* low-energies would impact the cells. However, this single energy experiment was done to higher fluences than would be seen per energy on orbit – giving good indication as to the expected degradation profile from combined low-energy protons. The results are consistent with the bare IMM flight degradation in **Figure 13**a.

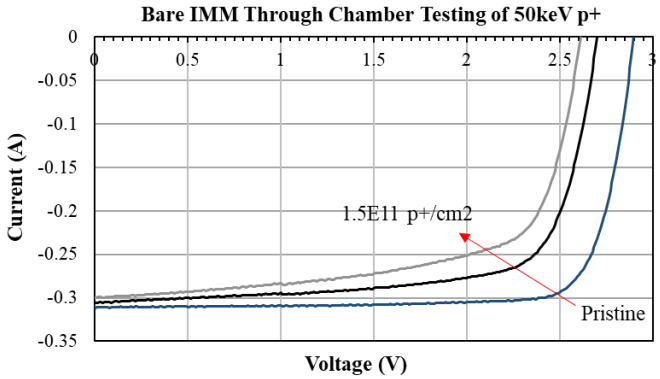

Figure 14: I-V data of a bare IMM cell through ground testing of trapped protons at 50keV. Pristine, 7.1x10^{10} p^{+}/cm^{2}, and 1.5x10^{11} p^{+}/cm^{2} shown.

Optinox SR IMM Assemblies: The addition of an Optinox SR coating to the IMM cells did not result in a significant improvement to power remaining at the end of the LEO mission. However, the coating did change the degradation profile, giving valuable insight into degradation methods and future direction for coating materials engineering. As observed in **Figure 13b** and **Table 2** the ending I_{sc} of Optinox SR IMM was signficatly *lower* than bare IMM while both the V_{oc} and FF were signifcantly *higher*. The latter is consistent with the coating providing protection from the low energy proton radiation. **Figure 15** highlights this, showing very little degrdation in power remaiming of ground tested Optinox coated IMM assemblies under 50keV protons and the same fluences as that shown in **Figure 14**.

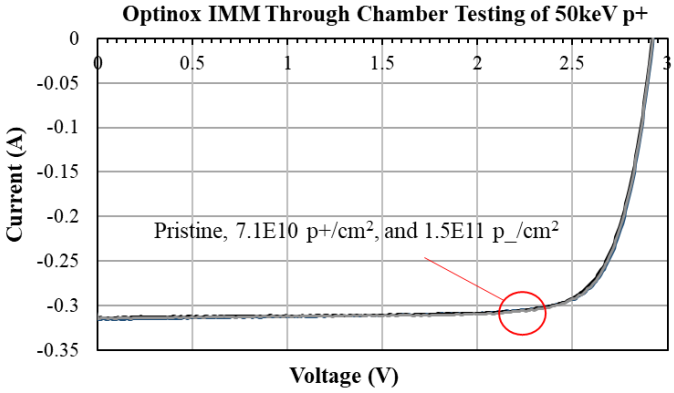

Figure 15: I-V data of a Optinox SR coated IMM cell through ground testing of trapped protons at 50keV. Pristine, 7.1x10^{10} p^{+}/cm^{2}, and 1.5x10^{11} p^{+}/cm^{2} shown.

The decreased I_{sc} is again expected to be caused by UV induced yellowing of the Optinox coating. While highly UV durable, a 1mil film of Optinox still has a 50% transmission cutoff around 288nm. **Figure 16** shows the ground tested I-V data of an Optinox coated IMM cell through 2,000 hours of UV exposure. Minor changes in the V_{oc} and FF were noted (<1%) with significant degradation in the I_{sc} (~16%); consistent with the flight samples. Thus, while Optinox blocked highly damaging low energy protons, it yellowed too quickly provide any net gain in end-of-life performance.

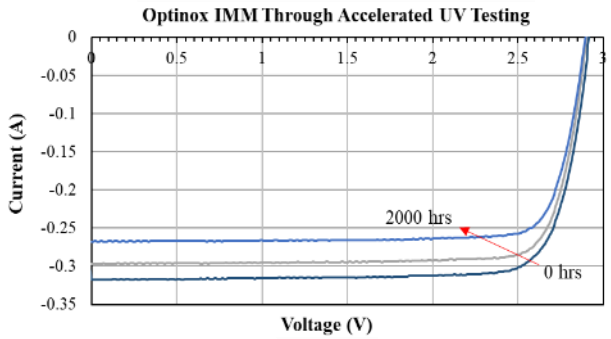

Figure 16: I-V data of a Optinox SR coated IMM cell through accelerated ground testing of UV exposure.

Optinox SR w/ POSS IMM Assemblies: Performance of the Optinox SR with POSS additive coated IMM cells was similar to that of straight Optinox SR. The addition of POSS, however, caused a further decrease in I_{sc} and a nearly equivalent increases in FF. While Optinox SR with POSS coating cells have not been ground tested, pre and post images show some slight hazing (**Figure 17**) to the exposed area of the coating. This is similar to that of CORIN XLS with Glass coated CIGS, but not nearly as pronounced. This haze is again attributed to neutral AO interaction with the POSS doping and reduces light transmission to the cell, accounting for the additional loss in current.

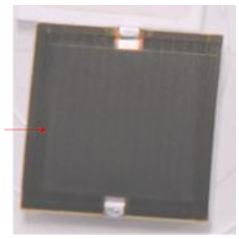

Figure 17: Enlarged image of Optinox SR with POSS coated IMM post-flight. Coloring enhanced to highlight hazing. Note, the unaffected area is that which was mounted under the plate lip and not exposed to AO.

4. CONCLUSIONS

The best performing CIGS assemblies, those with a CORIN XLS coating, showed 92.2% power retention after the 1-year (6,000 hours open and exposed) mission. The primary degradation of bare, uncoated CIGS modules in the LEO environment was found to be a combination of AO and UV. Adding the CORIN XLS coating significantly improved AO robustness and moderately improved UV resistance. While the CORIN XLS yellowed under UV, degrading I_{sc}, it did so more slowly than the V_{oc} and FF degradation of UV on bare modules – providing a net gain. The CIGS cell itself is robust to radiation damage, especially to the low fluences seen in LEO. A larger degree of performance variation was noted within the CIGS assemblies, indicating the need for tighter manufacturing controls. This work shows that CIGS assemblies, like those flown herein, can perform well for shorter term LEO missions, especially those with a higher risk tolerance, while further manufacturing control and qualification data is developed. To improve performance within LEO for longer duration, less risk-tolerant architectures, thin-film coatings that are robust to AO erosion *as well as UV* radiation are needed. This can be accomplished by coupling the CORIN XLS coating [or similar] with UV blocking, reflecting, or even down-converting [25, 26] schemes. Coatings that are optically clear through the entire UV band are not an option for CIGS modules as the UV radiation damages the CIGS cells themselves. Beyond LEO, this data again indicates the potential for CIGS assemblies to be utilized for shorter-term, higher risk mission classes. Atomic oxygen is a concern only to about 1,000km; however, beyond this particulate radiation then begins to increase. To improve CIGS assemblies for missions beyond LEO, coating development can neglect AO, however, should again focus on UV robustness as well as take appropriate considerations for higher fluences of low energy protons.

The best performing IMM assemblies, those with an Optinox SR coating, showed 79.0% power retention after the mission. However, there was not a significant difference between the power retention of uncoated, Optinox SR coated, and Optinox SR w/POSS coated assemblies. The primary degradation of the bare, uncoated IMM in LEO was found to be low-energy proton radiation. The addition of the Optinox SR coating significantly improved radiation robustness, however, suffered from significant UV radiation yellowing. Ultimately yielding similar power retention performance. Similar to the CIGS assemblies, IMM assemblies appear to be viable for shorter term, higher risk missions within LEO and beyond. Longevity improvements should again focus on thin-film, flexible coatings that are more robust to UV. Coatings that are optically clear through the entire UV band and/or down-converting assemblies are preferred for the IMM as these cells utilize a portion of the UV band for power conversion. IMM cells are much more sensitive to particulate radiation, especially low-energy protons, and coatings must account for this.

REFERENCES

[1] Yost, B., and Weston, S. "State-of-the-art small spacecraft technology." Vol. 20220018058, NASA NTRS, 2022.

[2] Weston, S., Miller, C. S., Ingersoll, J. E., Yost, B. D., Agasid, E., Burton, R., Carlino, R., Defouw, G., Perez, A. D., and Karacalioglu, A. G. "State of the art: Small spacecraft technology." Vol. 20200001421, NASA NTRS, 2020.

[3] Agasid, E., Burton, R., Carlino, R., Defouw, G., Perez, A. D., Karacalioglu, A. G., Klamm, B., Rademacher, A., Schalkwyck, J., and Shimmin, R. "Small spacecraft technology state of the art." NASA Technical Reports, 2015.

[4] Swartwout, M. "Twenty (plus) years of university-class spacecraft: A review of what was, an understanding of what is, and a look at what should be next," *Small Satellite Conference*. Logan, UT, 2006.

[5] Baker, D. N., and Worden, S. P. "The large benefits of small-satellite missions," *EOS, Transactions American Geophysical Union* Vol. 89, No. 33, 2008, pp. 301-302. doi: https://doi.org/10.1029/2008EO330001

[6] Simburger, E. J., Matsumoto, J. H., Giants, T. W., Garcia III, A., Liu, S., Rawal, S. P., Perry, A. R., Marshall, C. H., Lin, J. K., and Scarborough, S. E. "Thin-film technology development for the PowerSphere," *Materials Science and Engineering: B* Vol. 116, No. 3, 2005, pp. 265-272. doi: http://dx.doi.org/10.1016/j.mseb.2004.09.035

[7] Zuckermandel, J. W., Enger, S., Gupta, N., and Summers, J. "Modular, thin film solar arrays for operationally responsive spacecraft," *2007 IEEE Aerospace Conference*. IEEE, Big Sky, MT, 2007, pp. 1-6.

[8] Breen, M. L., Streett, A., Cokin, D., Stribling, R., Mason, A., and Sutton, S. "IBIS (Integrated Blanket/Interconnect System), Boeing's solution for implementing IMM (Inverted Metamorphic) solar cells on a light-weight flexible solar panel," *2010 35th IEEE Photovoltaic Specialists Conference*. IEEE, Honolulu, HI, 2010, pp. 000723-000724.

[9] Lichodziejewski, D., Veal, G., Helms, R., Freeland, R., and Kruer, M. "Inflatable rigidizable solar array for small satellites," *44th AIAA/ASME/ASCE/AHS/ASC Structures, Structural Dynamics, and Materials Conference*. Norfolk, VA, 2003, p. 1898.

[10] Reed, K., and Willenberg, H. J. "Early commercial demonstration of space solar power using ultra-lightweight arrays," *Acta Astronautica* Vol. 65, No. 9-10, 2009, pp. 1250-1260. doi: http://dx.doi.org/10.1016/j.actaastro.2009.03.055

[11] Iles, P. A. "Evolution of space solar cells," *Solar Energy Materials and Solar Cells* Vol. 68, No. 1, 2001, pp. 1-13. doi: https://doi.org/10.1016/S0927-0248(00)00341-X

[12] Chamberlain, M. K., Kiefer, S. H., LaPointe, M., and LaCorte, P. "On-orbit flight testing of the Roll-Out Solar Array," *Acta Astronautica* Vol. 179, 2021, pp. 407-414. doi: https://doi.org/10.1016/j.actaastro.2020.10.024

[13] Lockett, T. R., Martinez, A., Boyd, D., SanSoucie, M., Farmer, B., Schneider, T., Laue, G., Fabisinski, L., Johnson, L., and Carr, J. A. "Advancements of the lightweight integrated solar array and transceiver (LISA-T) small spacecraft system," *2015 IEEE 42nd Photovoltaic Specialist Conference (PVSC)*. IEEE, New Orleans, LA, 2015, pp. 1-6.

[14] Carr, J. A., Boyd, D., Martinez, A., SanSoucie, M., Johnson, L., Laue, G., Farmer, B., Smith, J. C., Robertson, B., and Johnson, M. "The Lightweight Integrated Solar Array and Transceiver (LISA-T): second generation advancements and the future of SmallSat power generation," *Small Satellite Conference*. Logan, UT, 2016.

[15] Carr, J. A., Johnson, L., Boyd, D., Phillips, B., Finckenor, M., Farmer, B., and Smith, J. C. "LISA-T part three: The design and space environments testing of a thin-film power generation and communication array," *Acta Astronautica* Vol. 205, 2023, pp. 267-280. doi: https://doi.org/10.1016/j.actaastro.2023.02.001

[16] De Groh, K. K., and Banks, B. A. "MISSE-Flight Facility Polymers and Composites Experiment 1-4 (PCE 1-4)." 2021.

[17] Reinhard, P., Chirilă, A., Blösch, P., Pianezzi, F., Nishiwaki, S., Buechelers, S., and Tiwari, A. N. "Review of progress toward 20% efficiency flexible CIGS solar cells and manufacturing issues of solar modules," *2012 IEEE 38th Photovoltaic Specialists Conference (PVSC) PART 2*. IEEE, 2012, pp. 1-9.

[18] Kirk, A., Cardwell, D., Wood, J., Wibowo, A., Forghani, K., Rowell, D., Pan, N., and Osowski, M. "Recent progress in epitaxial lift-off solar cells," *2018 IEEE 7th World Conference on Photovoltaic Energy Conversion (WCPEC)(A Joint Conference of 45th IEEE PVSC, 28th PVSEC & 34th EU PVSEC)*. IEEE, Waikoloa, HI, 2018, pp. 0032-0035.

[19] Heynderickx, D., Quaghebeur, B., Speelman, E., and Daly, E. "ESA's SPace ENVironment Information System (SPENVIS): a WWW interface to models of the space environment and its effects." 2000.

[20] Reddy, M. R., Srinivasamurthy, N., and Agrawal, B. "Atomic oxygen protective coatings for Kapton film: a review," *Surface and Coatings Technology* Vol. 58, No. 1, 1993, pp. 1-17.

[21] Buczala, D. M., Brunsvold, A. L., and Minton, T. K. "Erosion of Kapton H® by hyperthermal atomic oxygen," *Journal of spacecraft and rockets* Vol. 43, No. 2, 2006, pp. 421-425.

[22] Granata, J., Sahlstrom, T., Hausgen, P., Messenger, S., Walters, R., Lorentzen, J., Liu, S., and Helizon, R. "Thin-film photovoltaic proton and electron radiation testing for a meo orbit," *2006 IEEE 4th World Conference on Photovoltaic Energy Conference*. Vol. 2, IEEE, Waikoloa, HI, 2006, pp. 1773-1776.

[23] Imaizumi, M., Matsuda, S., Kawakita, S., Sumita, T., Takamoto, T., Ohshima, T., and Yamaguchi, M. "Activity and current status of R&D on space solar cells in Japan," *Progress in Photovoltaics: Research and Applications* Vol. 13, No. 6, 2005, pp. 529-543. doi: http://dx.doi.org/10.1002/pip.644

[24] Wright, J. S., Jones, A., Farmer, B., Rodman, D. L., and Minton, T. K. "POSS-enhanced colorless organic/inorganic nanocomposite (CORIN®) for atomic oxygen resistance in low earth orbit," *CEAS Space Journal*, 2021, pp. 1-15. doi: https://doi.org/10.1007/s12567-021-00347-7

[25] Darwish, A. M., Sarkisov, S. S., Patel, D. N., Fedoseev, A., Rossmanith, D., Grayol, B., Hirbljan, A., Koplitz, B., and El Rashedy, R. "Ultraviolet spectrum downshifting in polymer nanocomposite films for the enhancement of optoelectronic devices," *Photonic Fiber and Crystal Devices: Advances in Materials and Innovations in Device Applications XVII*. Vol. 12682, SPIE, 2023, p. 1268203.

[26] Darwish, A. M., Sarkisov, S. S., Graycol, B., Hribljan, A., Patel, D. N., Fedoseyev, A., Hui, D., Mele, P., Latronico, G., and Cho, K. "Polymer nanocomposite for protecting photovoltaic cells from solar ultraviolet in space," *Nanotechnology Reviews* Vol. 13, No. 1, 2024, p. 20240013. doi: https://doi.org/10.1515/ntrev-2024-0013